Liquid Crystals
Publication details, including instructions for authors and subscription information:
http://www.informaworld.com/smpp/title~content=t713926090

Nature of disclination cores in liquid crystals

Shanju Zhang[a]; Eugene M. Terentjev[a]; Athene M. Donald[a]
[a] Cavendish Laboratory, University of Cambridge, CB3 0HE, Cambridge, UK

To cite this Article Zhang, Shanju , Terentjev, Eugene M. and Donald, Athene M.(2005) 'Nature of disclination cores in liquid crystals', Liquid Crystals, 32: 1, 69 — 75
To link to this Article: DOI: 10.1080/02678290512331324057
URL: http://dx.doi.org/10.1080/02678290512331324057

Liquid Crystals, Vol. 32, No. 1, January 2005, 69–75

Taylor & Francis
Taylor & Francis Group

Nature of disclination cores in liquid crystals

SHANJU ZHANG, EUGENE M. TERENTJEV* and ATHENE M. DONALD
Cavendish Laboratory, University of Cambridge, Madingley Road, CB3 0HE, Cambridge, UK

(*Received 2 April 2004; in final form 16 August 2004; accepted 25 August 2004*)

A disclination is an orientation symmetry-breaking defect and its strength corresponds to the number of rotations (in multiples of 2π) of the director over a path encircling the disclination. The line core plays a considerable role in the disclination energy balance and mobility, however, the detailed nature of the core structure is largely unknown. Here we demonstrate different core structures for different disclinations by using transmission electron microscopy and atomic force microscopy coupled with the nanostripe decoration technique. We show that the molecular distribution in the core of (+1) defects changes from the prolate planar to oblate homeotropic, resembling but not identical to 'escape into the third dimension'. The homeotropic (−1) defect appears to possess an isotropic core, contrary to theoretical predictions.

1. Introduction

Studies of disclinations and their cores in small molecule nematic liquid crystals (LCs) have received great interest because of their fundamental role in physics of ordered media [1, 2] and their important effect on physical properties, e.g. the alignment quality or rheological behaviour [3, 4]. Generally, the core is considered to be the region of the topological defect where the elastic energy density of director gradients is so high that the local order parameter deviates significantly from the asymptotic value required by the bulk thermodynamic state. On the basis of Landau–de Gennes theory, the nematic material inside the disclination core not only shows a decrease in the degree of orientation but also switches from uniaxial to biaxial order to reduce the elastic energy of director gradients [5–7]. The core size has been estimated to be of the order of tens of nanometers, depending on the nature of materials. Numerical simulation of the details of the core structure confirms this structure with biaxial ordering [8–11]. Experimentally, early studies of the defect core were conducted with optical microscopy [12, 13]. Although the direct core structure cannot be resolved with optical methods, the differences between negative and positive disclinations have been identified and explained by the different densities of chain ends aggregated in the core [12]. More recently, transmission electron microscopy (TEM) was applied to study the disclinations and the near-core structure of disclinations was then analysed in terms of the apparent splay and bend elastic anisotropy [14]. However, to the best of our knowledge the inner core structure of a disclination has never been directly visualized.

Recently, we reported the observation of two-dimensional nanoscale stripes in thin films of a side chain smectic polymer using TEM and atomic force microscopy (AFM) [15]. When the samples were cooled to the smectic phase, after a holding period in the nematic phase, a characteristic surface morphology developed. This morphology manifested itself in bright field TEM and the height- or phase-contrast AFM images as a series of nanostripes aligned with the local director axis. This orientation was demonstrated by correlating the direction of the stripes with electron diffraction patterns. The stripes were shown to result from an effect analogous to the Rayleigh–Taylor instability, in this case arising due to the competition between the layer-aligning effect of the substrate and the planar director alignment, which would force smectic layers to line up perpendicular to the film surface. Stripes serve to decorate the underlying molecular alignment, yielding a high resolution map of director fields over length scales down to tens of nanometers, but do not rely on any crystallization of the polymer, nor staining or etching, unlike previous techniques for observing director fields [16, 17].

In this work, we extend this nanostripe decoration technique to study the disclination core by TEM and AFM. The polymer in this work is an end-on fixed side group liquid crystalline polysiloxane, in which the mesogenic rod-like molecular moiety is attached to the flexible backbone at one end. Its chemical structure is

*Corresponding author. Email: emt1000@cam.ac.uk

Liquid Crystals ISSN 0267-8292 print/ISSN 1366-5855 online
http://www.tandf.co.uk/journals
DOI: 10.1080/02678290512331324057

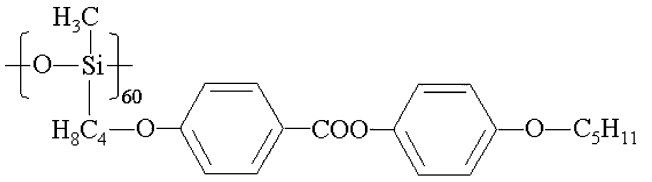

The material was prepared in-house, following the well known procedure of hydrosilylation reactions with polysiloxanes [18, 19]. Its phase behaviour was studied by differential scanning calorimetry (DSC) and polarizing optical microscopy (POM). The polymer has a glass transition (T_g) at 12°C, a smectic–nematic transition at 82°C and a nematic–isotropic transition (T_{NI}) at 97°C. The phases were identified by characteristic textures observed under by POM.

2. Experimental

Thin films with thickness of *c*. 50 nm were prepared by spin-coating on carbon-coated mica from a 1% chloroform solution of the polymer at a speed of 3000 rpm. After complete solvent evaporation, the films were annealed in an oven at 90°C (to the nematic phase) for 10 h to develop the defect texture, and subsequently quenched to room temperature by setting the mica on a metallic plate. The quenched samples were directly used for AFM investigation. For TEM investigation, the thin films were stripped, floated on a water surface, and collected on TEM copper grids.

The microstructures and morphologies of thin films were observed using a TECNAI-20 TEM at an accelerating voltage of 120 kV. The samples were examined without staining or shadowing under TEM. The defocusing technique only was used to obtain the contrast in the images [15]. The AFM images were obtained using a Nanoscope IIIa scanning probe microscope (Digital Instruments Dimension 3100) operated in tapping mode under ambient conditions. A single crystal silicon probe tip was used. Images of each sample were recorded in height- and phase-contrast modes, and analysed with the Nanoscope image processing software.

3. Results and discussion

We started with thin (*c*. 50 nm thick) films of the polymer prepared by spin-coating the polymeric solution on the carbon surface. Observed under TEM, the typical morphologies and structures around the four types of $s=\pm1$ disclinations in isolation are revealed by nanostripes at a high resolution, as shown in figure 1. As the director of the mesogenic groups is parallel to the direction of the stripes, the orientation of stripes reveals the actual trajectories of the director around each disclination [15]. One can immediately observe the pattern of contrasting stripes, which evidently follow the director pattern around each disclination. We found only one type of disclination with strength $s=-1$. This has a hyperbolic structure (H) with fourfold symmetry, figure 1 (*a*), while disclinations with strength $s=+1$ have three different patterns of director field: radial (R), circular (C), and spiral patterns (S); figures 1(*b–d*). These patterns can be distinguished by a parameter *c*, which relates the axial position in the plane around the disclination core (polar angle θ) and the director orientation angle ϕ: in the simplest case $\phi(\theta)=s\theta+c$, as described by Frank continuum theory [20]. According to this theory, one negative pattern and three positive patterns can be expected in a two-dimensionally ordered liquid crystal, as observed here. Radial and circular patterns occur when the constant *c* is 0 and $\pi/2$, respectively. For other values of *c*, between $-\pi/2$ and $\pi/2$, spiral patterns occur. It is interesting to note from the images that the cores of ±1 disclinations are around 80 nm in diameter, and the TEM images therefore provide sufficient resolution to examine the different core structures directly. The positive disclinations with $s=+1$ (radial (R), circular (C) and spiral (S) patterns) have circular dark regions at their core, while the hyperbolic (H) pattern of the negative disclination with $s=-1$ exhibits a bright central region. Moreover, there are small differences among the positive disclination

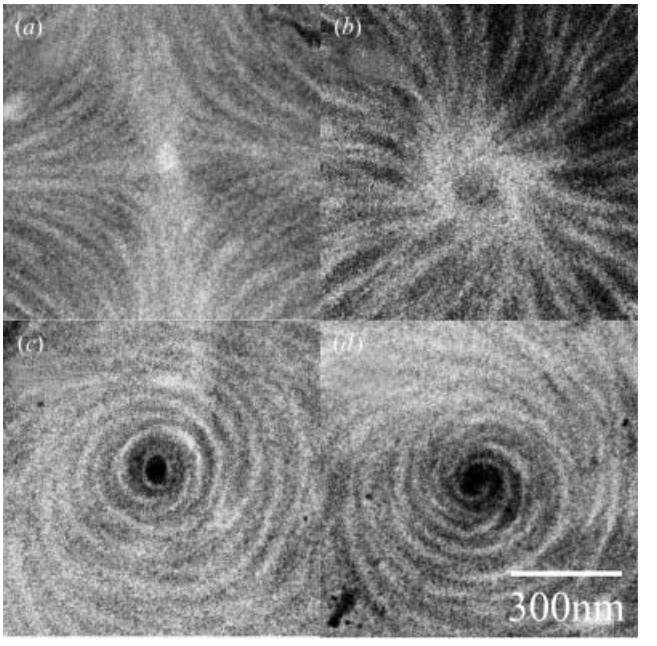

Figure 1. A series of TEM micrographs showing the different types of integer disclinations. (*a*) Hyperbolic pattern (H), $s=-1$; (*b*) radial pattern (R), $s=+1$, $c=0$; (c) circular pattern (C), $s=+1$, $c=\pi/2$; (*d*) spiral pattern (S), $s=+1$, $0<c<\pi/2$.

cores. The R core is dark with bright edges. The C core seems darker than the S core, which is itself darker than the R core. In our previous work [15], we argued that dark regions in the TEM bright field image could result from two possible sources of contrast: (1) the director orientation moving out of the film plane leading to increased scattering out of the bright field image [21] and (2) thickness variations in the polymer film. Thus, the contrast differences among integral disclination cores in this work can provide detailed insight into the core structure, discussed in terms of the effect of different director orientations and/or thickness variations.

Figure 2 shows AFM images of four configuration patterns of ± 1 disclinations in height-contrast and phase-contrast modes. The core regions of all four configurations in AFM height-contrast images appear dark, indicating (since this imaging mode provides an unambiguous interpretation of the contrast in terms of local film thickness) that the core regions of all four configurations are thinner than the surrounding material. The height differences are found to vary from 2 to 8 nm, largely depending on the configuration patterns. As shown in figure 3, H and R cores have a depth of *c*. 8 nm while C and S cores are *c*. 2.5 nm deep. The corresponding phase-contrast images of the three positive disclinations show similar core sizes in each case to the height-contrast results, whilst the core of the $s=-1$ (H) disclination in the phase image is seen to be much smaller than that in the corresponding height contrast. The thinner polymer film at the cores of positive and negative disclinations should (if thickness variations are the main source of image contrast in the TEM) allow more electrons to penetrate the film and hence give bright domains in TEM bright field images. In fact, this is not what is seen in figure 1, where all three of the $s=+1$ disclinations exhibit dark cores. Thus, TEM and AFM results, when combined, indicate that it is variations of the director orientation, that mainly give rise to the differences in TEM contrast between positive and negative disclination cores. This would be consistent with the idea of mesogenic groups tilting out of the plane of the film within the core, for both types of disclinations (escape into the third dimension) [22]. For the $s=+1$ case, diffraction contrast due to the average mesogen orientation appears to dominate in the TEM image, leading to the central region looking dark. Conversely, for the $s=-1$ disclination, the thinning of the material within the core dominates, leading to its bright TEM appearance, presumably either because the tilt of the molecules is less in this case, or more likely the packing of mesogens is less ordered.

It should be noted that in phase-contrast AFM images the bright part of the core in H and R disclinations does not correspond precisely to the actual structure of the core itself. In order to investigate this question in greater detail, we have separately studied a region in the thin polymer film where the director is aligned nearly uniformly (no disclination) but the film itself had a defect – a 'hole' of about 25 nm deep. Figure 4 shows the results of AFM scans across such a hole in the height-contrast and phase-contrast regimes. In the latter case we clearly see that the phase contrast can be markedly different depending on whether the AFM tip is climbing or descending into the hole. In the trace-recording, which means the AFM tip moves from

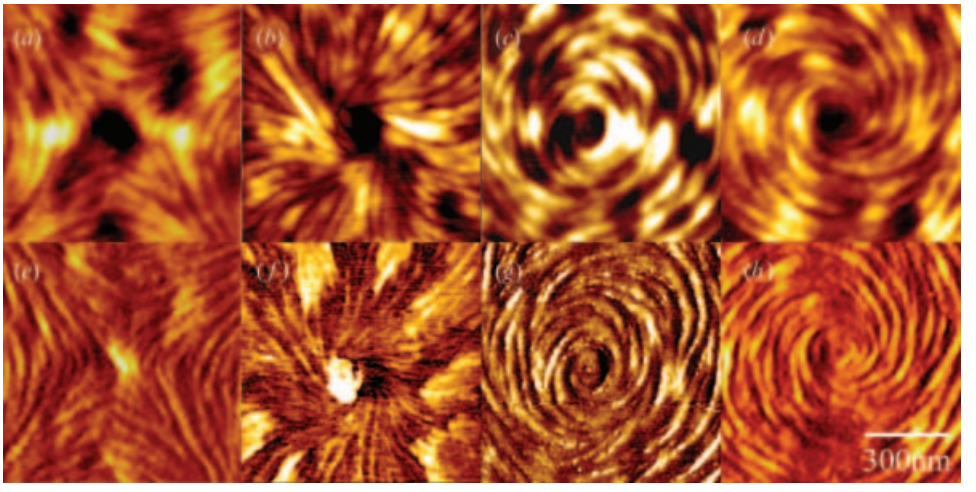

Figure 2. A series of AFM images of the different types of integer disclinations in height-contrast (top) and phase-contrast (bottom). All cores show dark regions in height-contrast AFM images, indicating that the film surface in each core is lower than in the surrounding area. This, combined with the dark TEM contrast, points to the idea of mesogenic groups tilting out of the plane of the film within the core. sequences (*a–d*) and (*e–h*) correspond to sequence (*a–d*) in figure 1.

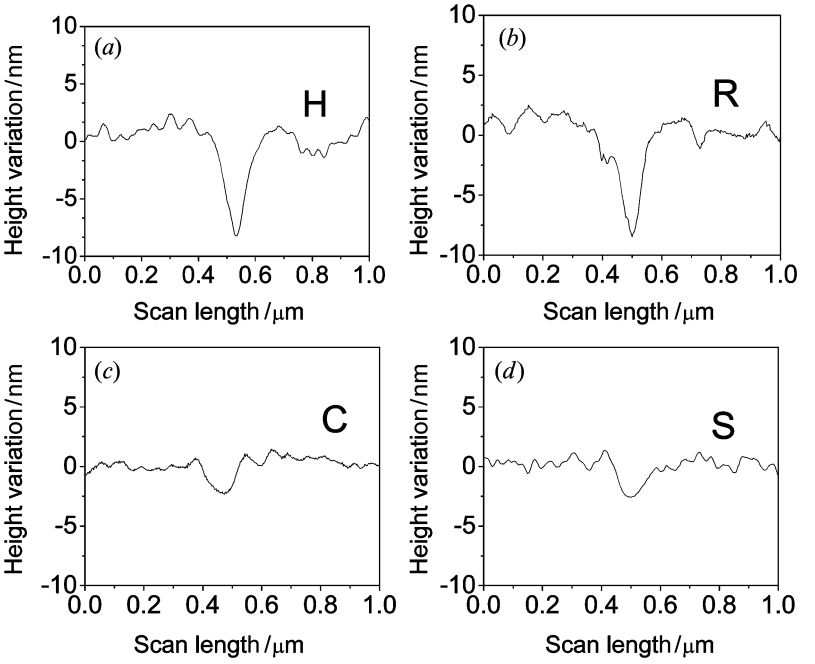

Figure 3. Height variations across the disclination cores from the AFM height images. (*a*) Hyperbolic pattern (H), $s=-1$; (*b*) radial pattern (R), $s=+1$, $c=0$; (*c*) circular pattern (C), $s=+1$, $c=\pi/2$; (*d*) spiral pattern (S), $s=+1$, $0<c<\pi/2$. H and R cores have about 8 nm depths while C and S cores are about 2.5 nm deep.

'left to right' in figure 4 (*c*), the image contrast is bright on the left of the hole, while on the right in the retrace-recording—the AFM tip moves from 'right to left' as shown in figure 4 (*d*)—the contrast is preserved. Under the tapping mode, when the tip encounters a low point in the sample the tip coming down into the pit will feel more attraction and form a stiffer contact than a tip moving out of the pit [23]. Apparently, the bright part of phase-contrast images results from the mechanical response when the AFM tip moves abruptly from the high to the low, corresponding to some type of 'overshoot' phenomenon. This suggests that the bright parts in H and R cores result from a similar mechanism. For our system, this artefact always occurs when the pit depth is larger than 5 nm. It is interesting to note that although the film in disclination cores in this work is always thinner than the surrounding material, the pit itself is not necessarily a nucleating agent for the growth of a disclination. As shown in figure 4, the director orientation could remain uniform and unaffected by an accidental hole. On the other hand, it is easy to imagine that the polymer film in the annealed nematic state would become thinner to reduce the amount of material in the region of high energy density (core). Our results reflect the unique characteristic of a pit core in a topological defect and the complex formation process of a disclination.

So, combining the information obtained from the three methods of analysis, we conclude that all

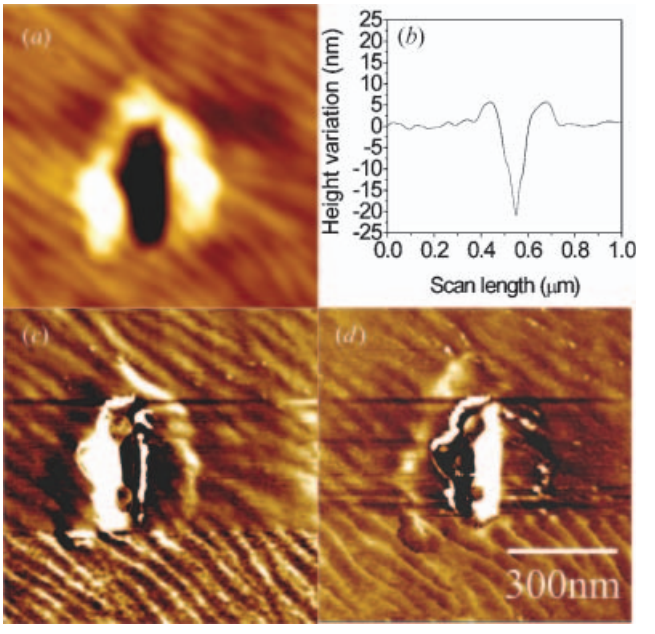

Figure 4. A series of AFM images across the hole. (*a*) Height-contrast image showing the uniform stripes around the hole. (*b*) The scan of height variation across the hole from (*a*)–(*c*) Trace-recording (from left to right) phase-contrast image showing the bright part in the left of the hole. (*d*) Retrace-recording (from right to left) phase image showing the bright part in the right of the hole. The bright region in the hole results from the mechanical response when the AFM tip moves abruptly from the high to the low.

disclination cores are associated with a local depression of the free film thickness. This, on its own, would have resulted in bright TEM contrast. However, apart from the H disclination, figure 1 (*a*), all cores have dark contrast. This can only be explained by enhanced attenuation of the primary electronic beam passing through a region with locally homeotropic (or nearly so) director alignment. In this case the high polarizability of conjugated electrons on the mesogenic groups would scatter the beam, in spite of the path length through the sample being apparently lower—resulting in the dark cores of +1 disclinations. The case of −1 disclination is different: the TEM shows the bright contrast consistent with the reduced thickness and non-specific orientation of mesogenic groups; that the core of an H defect is isotropic is a natural conclusion.

How does this correspond to what is known about disclination cores based on the continuum mean-field theory? The general biaxial nematic order parameter is $Q_{ij}=Q\ (n_in_j-\delta_{ij}/3)+P(m_im_j-l_il_j)/3$, with **n** the main director and **m,l** the other principal axes of the biaxial order, the strength of which is measured by the parameter P. In the bulk uniaxial nematic phase $P=0$. In the Landau–de Gennes theory, the free energy density of a nematic LC is expressed in the rotationally-invariant form

$$F = a\ Q_{ij}\ Q_{ji} - b\ Q_{ij}Q_{jk}Q_{ki} + c\left(Q_{ij}Q_{ji}\right)^2 + L\ \nabla_k Q_{ij}\ \nabla_k Q_{ij} \qquad (1)$$

where $a=a_0(T-T^*)$, b,c are positive constants (for a rod-like nematic) describing thermodynamically equilibrium nematic order, and L is the elastic constant in a simplifying one-constant approximation; it is related to the bulk Frank constant as $K=LQ^2$. In the bulk, the thermodynamic part of the free energy density penalizes deviations from the equilibrium uniaxial order Q_0, which is obtained by direct minimisation of equation (1) giving

$$Q_0 = \frac{3b}{16c}\left[1+\left(1-\frac{64ac}{3b^2}\right)^{\frac{1}{2}}\right] \sim (3b/8c). \qquad (2)$$

The thermodynamic free energy penalty for deviations from Q_0 is relatively very high:

$$\Delta F_{\mathrm{TD}} = \frac{b^2}{16c}\left[1+\left(1-\frac{64ac}{3b^2}\right)^{\frac{1}{2}}-\frac{64ac}{3b^2}\right][Q-Q_0]^2 \sim \left(b^2/8c\right)[Q-Q_0]^2. \qquad (3)$$

These are the classical results of basic Landau–de Gennes treatment of nematic ordering. In both expressions, the second (approximate) form is an order of magnitude estimate based on the assumption that the temperature-dependent combination of Landau coefficients under the square root is of order one, sufficiently far from the clearing point. The main point of this estimate is to get the impression, as to whether or not the observed core radius is determined by the balance of nematic free energy contributions, as in low molar mass liquid crystals.

Close to the defect centre, the energy density of elastic distortions increases so much that it becomes comparable with ΔF_{TD} and leads to significant changes in local nematic order, which we identify as the disclination core. As a result the core size can be estimated by matching the bulk thermodynamic penalty, equation (3) and the free energy density of elastic distortions in the region of $Q=Q_0$: $\Delta F_{\mathrm{el}}\sim(2/3)LQ_0^2/r_{\mathrm{core}}^2$. This gives

$$r_{\mathrm{core}} \approx \left(\frac{16c}{3b^2}\right)^{\frac{1}{2}}\frac{L^{\frac{1}{2}}Q_0}{|Q-Q_0|} \sim \frac{\left(3Kc/b^2\right)^{\frac{1}{2}}}{|Q-Q_0|} \qquad (4)$$

where, as before, $K=LQ^2$. In the quoted literature one can find a few more elaborate expressions of this radius, but the comparison with experiment will ultimately be limited by our incomplete knowledge of phenomenological parameters entering any such theory. We therefore choose a more basic estimate, which should give the correct order of magnitude as long as the underlying physical mechanism is captured correctly. Note that exactly the same argument stands for defining the nematic correlation length ξ, far from the transition point into the isotropic phase, and so the disclination core size is proportional to ξ apart from a numerical coefficient of order of unity.

The estimate of Frank elastic constant, $K\sim10^{-11}$ N, is quite robust. This value is dictated by basic dimensional analysis and is indeed found in most liquid crystals, including polysiloxane side chain polymers similar to our system [24]. Deciding on the correct values for Landau coefficients is a somewhat ambiguous task. One could find some estimates in the literature [25], or deduce the three parameters (a_0, b, c) from the three independent measurements of: (i) the jump of the order parameter $\Delta Q_0=3b/16c$ at the nematic–isotropic transition ($\sim$0.4, so $b\sim2c$); (ii) the width of the transition hysteresis $|T^*-T_{\mathrm{NI}}|=b^2/4a_0c$ (usually less than 1°, so $a_0\sim c/1$ K); and (iii) the enthalpy of this weak first order transition $\Delta H=T_{\mathrm{NI}}b^2/4a_0c$ ($\sim$1–2 J g^{-1}, when $T_{\mathrm{NI}}\sim$ 300 K), see [26] for an example of such deduction. As a result, one finds $b\sim3.1\times10^6$ J m^{-3} and $c\sim1.4\times10^6$ J m^{-3}. Substituting these values, and K, into equation (4) and taking difference $|Q\text{-}Q_0|\sim0.5$, we obtain $r_{\mathrm{core}}\sim41$ nm. In our work, figures 1 and 2, the cores determined from TEM and AFM images, are seen to be roughly circular with radii of $\sim$40 nm. Considering

the order of magnitude level of this estimate, this is a very good agreement. Such a close correspondence suggests that we indeed have singular topological defects and not, as one might have expected for disclinations with integer strength $s=\pm 1$, macroscopic non-singular textures with the director 'escaped into the third dimension' [22]. In that case the angle of director deflection out of the sample plane would follow a power law $\sim r^{-s}$, which should show a broad and diffuse core image, while we observe narrow and sharply defined core regions of the size $r_{\text{core}}\sim\xi$. The fact that we see singular integer-strength disclinations in a nematic, where they are known to be topologically unstable [1, 2], is almost certainly due to the strong planar anchoring of the bulk nematic director **n** that is effectively confined to the film plane. Assuming such planar confinement, with $n_x\approx\cos(s\theta+c)$ and $n_y\approx\sin(s\theta+c)$, and the biaxial triad $m_x\approx$-$\sin(s\theta+c)$ and $m_y\approx\cos(s\theta+c)$, with $l_z\approx 1$, the free energy density (1) takes the form

$$F\approx\frac{2}{3}a\left(Q^2+\frac{1}{3}P^2\right)-\frac{2}{9}b\left(Q^3-P^2Q\right)+\frac{4}{9}c\left(Q^4+\frac{2}{3}P^2Q^2+\frac{1}{9}P^4\right)+\frac{2}{9}L\,s^2\frac{1}{r^2}(3Q-P)^2+\frac{2}{3}L\left[(Q')^2+\frac{1}{3}(P')^2\right] \quad (5)$$

where $Q'=\mathrm{d}Q/\mathrm{d}r$ and $P'=\mathrm{d}P/\mathrm{d}r$ describe, respectively, the variation of the main and the biaxial order parameters near the core (in the bulk these gradients vanish, $Q=Q_0$ and $P=0$). Minimization of this expression can be performed in three limiting cases:

(a) Assuming there is no order parameter variation at all. Then $Q=Q_0$, $P=0$ and $F\sim 2LQ^2s^2/r^2$.
(b) Assuming the uniaxial nematic order melts into the isotropic phase, $Q=Q(r)$, but $P=0$.
(c) Allowing arbitrary biaxial order to develop, $Q=Q(r)$ and $P=P(r)$.

Figure 5 shows the resulting plots of free energy density (the last two cases numerically), clearly indicating that the biaxial scenario is preferable, at least within the limitations of Landau–de Gennes theory. Also, there is clearly no dependence on the difference between disclinations with $s=\pm 1$. These are the conclusions of all authors who have written on this subject over the years [5–7]. Our observations present two major discrepancies with this description: defects with $s=+1$ may have some biaxiality developing in the core, but the main effect seems to be the switch to a well aligned homeotropic alignment within r_{core}. The defect with $s=-1$ shows a very different core structure, most consistent with the isotropic core model. We cannot attribute any of these facts to elastic anisotropy (Frank constants $K_1\neq K_3$, or the same with Landau expansion coefficients L_1 and L_2) because in our nematic polymers this anisotropy is very small indeed [27].

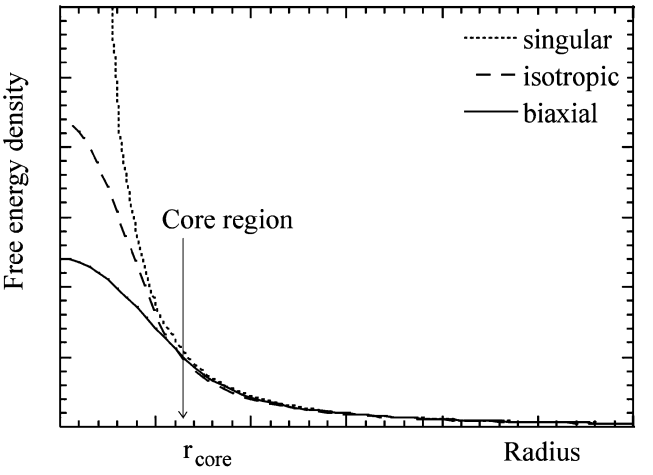

Figure 5. Model plots of free energy density as function of radius from the disclination line, for the three classical models of core structure based on the continuum mean-field theory.

4. Summary

We have directly visualized the disclination core structures of liquid crystal nematics in side chain polymer thin films by using the high resolution techniques of transmission electron microscopy and atomic force microscopy coupled with the nanostripe decoration technique. The experiments shown here support the core size estimate based on Landau–de Gennes theory. This theory provides a general framework for understanding how the symmetry is broken in topological defect cores, but disagrees with our observations in several important details. Knowing the core structure can shed light on defect mobility, which, in turn, affects both the deformation and relaxation behaviour of nematic liquids and polymers. Much remains to be understood in this area.

Acknowledgements

We would like to thank A.R. Tajbakhsh for kindly providing the polymers, and J. Adams, T.J. Sluckin, M. Kleman and E.L. Thomas for helpful discussions. The support of EPSRC is greatly appreciated.

References

[1] M. Kleman. *Points, Lines and Walls in Magnetics, Liquid Crystals and other Ordered Media*. John Wiley, New York (1983).
[2] V.P. Mineev. *Topologically Stable Defects and Solutions in Ordered Media*. Harwood Academic (1998).

[3] P.E. Cladis, W. van Saarloos, P.L. Finn, A.R. Kortan. *Phys. Rev. Lett.*, **58**, 222 (1987).
[4] W. Song, I.A. Kinlock, A.H. Windle. *Science*, **302**, 1363 (2003).
[5] I.F. Lyuksyutov. *Sov. Phys. JETP*, **48**, 178 (1978).
[6] N. Schopohl, T.J. Sluckin. *Phys. Rev. Lett.*, **59**, 2582 (1987).
[7] E. Penzenstadler, H.R. Trebin. *J. Phys.* (Fr.), **50**, 1027 (1989).
[8] P. Biscari, T.J. Sluckin. *Euro. J. appl. Math.*, **14**, 39 (2003).
[9] N.J. Mottram, S.J. Hogan. *Philos. Trans. r. Soc. A*, **355**, 2045 (1997).
[10] P.E. Biscari, G. Virga. *Int. J. non-lin. Mech.*, **32**, 337 (1997).
[11] S.D. Hudson, R.G. Larson. *Phys. Rev. Lett.*, **70**, 2916 (1993).
[12] G. Mazelet, M. Kleman. *Polymer*, **27**, 714 (1986).
[13] R.B. Meyer. *Mol. Cryst. liq. Cryst.*, **16**, 405 (1972).
[14] S.D. Hudson, J.W. Fleming, E. Gholz, E.L. Thomas. *Macromolecules*, **26**, 1270 (1993).
[15] S. Zhang, E.M. Terentjev, A.M. Donald. *Eur. Phys. J. E*, **11**, 367 (2003).
[16] B.A. Wood, E.L. Thomas. *Nature*, **324**, 655 (1986).
[17] D.L. Handlin Jr, E.L. Thomas. *Macromolecules*, **16**, 1514 (1983).
[18] H. Finkelmann, H.J. Kock, G. Rehage. *Macromol. rapid Commun.*, **2**, 317 (1981).
[19] B. McArdle. *Side Chain Liquid Crystal Polymers*. Blackie, Glasgow (1989).
[20] F.C. Frank. *Discuss. Faraday Soc.*, **25**, 19 (1958).
[21] A.M. Donald, A.H. Windle. *Polymer*, **25**, 1235 (1984).
[22] P.G. De Gennes, J. Prost. *The Physics of Liquid Crystals*. Clarendon Press, Oxford (1993).
[23] O.P. Behrend, L. Odoni, J.L. Loubet, N.A. Burnham. *Appl. Phys. Lett.*, **75**, 2551 (1999).
[24] J. Schmidtke, W. Stille, G. Strobl. *Macromolecules*, **33**, 2922 (2000).
[25] L.M. Blinov, V.G. Chigrinov. *Electrooptic Effects in Liquid Crystal Materials*. Springer, New York (1994).
[26] M. Warner, E.M. Terentjev. *Liquid Crystal Elastomers*. Clarendon Press, Oxford (2003).
[27] S. Zhang, E.M. Terentjev, A.M. Donald. *Macromolecules*, **37**, 390 (2004).